

1998

# Dynamic Path Integral Methods: A Maximum Entropy Approach Based on the Combined use of Real and Imaginary Time Quantum Monte Carlo Data

Dongsup Kim

J. D. Doll

*See next page for additional authors*

Follow this and additional works at: [https://digitalcommons.uri.edu/chm\\_facpubs](https://digitalcommons.uri.edu/chm_facpubs)

Terms of Use

All rights reserved under copyright.

---

## Citation/Publisher Attribution

Kim, Songsup, J. D. Doll and David L. Freeman. "Dynamic Path Integral Methods: A Maximum Entropy Approach Based on the Combined Use of Real and Imaginary Time Quantum Monte Carlo Data." *Journal of Chemical Physics*. 108(10):3871-3875. 8 March 1998.

This Article is brought to you for free and open access by the Chemistry at DigitalCommons@URI. It has been accepted for inclusion in Chemistry Faculty Publications by an authorized administrator of DigitalCommons@URI. For more information, please contact [digitalcommons@etal.uri.edu](mailto:digitalcommons@etal.uri.edu).

---

**Authors**

Dongsup Kim, J. D. Doll, and David L. Freeman

# Dynamic path integral methods: A maximum entropy approach based on the combined use of real and imaginary time quantum Monte Carlo data

Dongsup Kim and J. D. Doll

*Department of Chemistry, Brown University, Providence, Rhode Island 02912*

David L. Freeman

*Department of Chemistry, University of Rhode Island, Kingston, Rhode Island 02881*

(Received 20 October 1997; accepted 5 December 1997)

A new numerical procedure for the study of finite temperature quantum dynamics is developed. The method is based on the observation that the real and imaginary time dynamical data contain complementary types of information. Maximum entropy methods, based on a combination of real and imaginary time input data, are used to calculate the spectral densities associated with real time correlation functions. Model studies demonstrate that the inclusion of even modest amounts of short-time real time data significantly improves the quality of the resulting spectral densities over that achievable using either real time data or imaginary time data separately. © 1998 American Institute of Physics. [S0021-9606(98)51010-0]

## I. INTRODUCTION

The Monte Carlo method<sup>1,2</sup> has been applied to the finite temperature quantum dynamics problem in two basic ways. One approach is to utilize Monte Carlo methods (or their generalization) to calculate directly the required “real time” quantum dynamical correlation functions. Another approach is to obtain the required dynamical information “indirectly” using suitably designed, imaginary time equilibrium simulations. Both approaches have their own unique advantages and disadvantages.

In the direct approach, conventional Monte Carlo importance sampling methods are of limited use. The well known “sign problem” associated with the phase oscillations of the real time propagator,  $e^{itH/\hbar}$ , leads to exponentially growing variances as the time,  $t$ , increases.<sup>3-5</sup> If only very short time information is required, as would be the case if we were studying the flux autocorrelation functions for a simple barrier crossing event, then brute force Monte Carlo procedures may suffice.<sup>6</sup> If, however, longer time data are required, then more general approaches are necessary.

Many approaches have been proposed to defeat the sign problem.<sup>7-10</sup> While progress continues, the actual application of direct methods to realistic physical systems are, at present, rare.

In the indirect approach, the correlation functions in imaginary time are calculated by a usual equilibrium quantum Monte Carlo simulation method,<sup>3,4</sup> and the desired real time correlation functions are obtained by an analytic continuation procedure.<sup>11-13</sup> The main difficulty of this method is that the analytic continuation is numerically unstable so that the unavoidable statistical errors of the equilibrium Monte Carlo calculations are magnified in an uncontrollable way. Several different approaches to deal with the numerical instability associated with the analytic continuation have been proposed. Among those, the maximum entropy inver-

sion method<sup>14-18,23</sup> is the most recent and by far the most successful. It has been applied with success to problems such as quantum lattice models,<sup>14</sup> the solvated electron,<sup>16</sup> liquid <sup>4</sup>He,<sup>17</sup> and adsorbate vibrational lineshapes.<sup>18</sup> A major shortcoming of the maximum entropy method is that it requires extremely accurate imaginary time correlation functions to obtain converged results. This implies that it is often difficult to obtain high resolution dynamical detail.

In this paper we develop a new method which utilizes both imaginary time and real time quantum Monte Carlo data. The method is mainly based on the maximum entropy method, but unlike previous approaches, it uses both real and imaginary time data as input. In the next section, we indicate how the real time information can be included in the maximum entropy reconstruction scheme. We focus our attention on calculating the lineshape function,  $I(\omega)$ , in vibrational spectroscopy. Extension to the general quantum dynamics problem is straightforward. In Sec. III, we demonstrate the utility of our method on a few selected examples.

## II. FORMAL DEVELOPMENTS

A generic time correlation functions,  $C(t)$ , is related to its associated spectral density,  $I(\omega)$ , by means of a Fourier transform relationship

$$C(t) = \int_{-\infty}^{\infty} e^{-i\omega t} I(\omega) d\omega. \quad (1)$$

As documented elsewhere,<sup>14,15</sup> the corresponding imaginary time correlation function,  $G(\tau) \equiv C(-it)$ , can be written as

$$G(\tau) = \int_0^{\infty} K(\tau, \omega) I(\omega) d\omega, \quad (2)$$

where  $I(\omega)$  is the same spectral density that appears in Eq. (1) and  $K(\tau, \omega)$  is a known integral kernel. Of relevance for the present discussion is that  $K(\tau, \omega)$  tends to be a strongly decaying function of the frequency,  $\omega$ .

Although they share a common spectral density, the differences between kernels of Eqs. (1) and (2) have profound implications with respect to the way in which this density is “expressed.” Specifically, the strongly decreasing character of the integral kernel  $K(\tau, \omega)$  implies that  $G(\tau)$  preferentially contains information concerning the low-frequency components of  $I(\omega)$ . High frequency information is obtained only with some difficulty. On the other hand, the Fourier transform structure of Eq. (1) implies that  $C(t)$  preferentially provides information about the high frequency components of the spectral density. That is, if approached through  $C(t)$ , it is the long-time or low-frequency information that is difficult to obtain.

Within the dipole approximation, the vibrational lineshape,  $I(\omega)$ , can be obtained from the position autocorrelation function,<sup>19</sup>  $C(t) = \langle \mathbf{r}(t) \cdot \mathbf{r}(0) \rangle$  by Eq. (1), where  $\mathbf{r}(t)$  is the Heisenberg operator, i.e.,  $\mathbf{r}(t) = e^{itH/\hbar} \mathbf{r} e^{-itH/\hbar}$ , and  $\langle \dots \rangle$  is the thermal average,  $\langle \dots \rangle = \text{Tr}[e^{-\beta H} \dots] / Q$  with the partition function  $Q$ .  $H$  is the system’s Hamiltonian and  $\beta$  the inverse temperature,  $\beta = 1/kT$ .

$C(t)$  can be written in multidimensional integral form using Feynman’s path integral representation of the propagator.<sup>20,21</sup> The direct approach is to evaluate the multidimensional integral by Monte Carlo techniques with an appropriate importance sampling procedure. This approach may not, however, be the best one for the lineshape function calculation. For example, if  $I(\omega)$  contains low frequency components, one needs  $C(t)$  over a relatively long time in order to resolve them. This information is difficult to obtain since the complexity in the real time Monte Carlo calculation grows exponentially as a function of the time,  $t$ . Because  $C(t)$  must be truncated at some finite time,  $t_{\max}$ , and since it also contains the statistical errors, the Fourier transform usually gives artificial defects in  $I(\omega)$ , typically rapidly varying side lobes around peaks. Various forms of windowing functions have been used to prevent these phenomena.<sup>22</sup> Maximum entropy methods have also been used in Fourier transform for the same purpose. As demonstrated in the next section,  $I(\omega)$  calculated using maximum entropy method is much better than that of the usual numerical Fourier transform with the windowing functions.

The same lineshape function  $I(\omega)$  can be obtained by inverse Laplace transform of the imaginary time correlation function,  $G(\tau) \equiv C(-it)$ ,

$$G(\tau) = \int_{-\infty}^{\infty} e^{-\omega\tau} I(\omega) d\omega. \quad (3)$$

The numerical instability associated with the inverse Laplace transform is controlled by the maximum entropy method. Using the Bayesian approach of probability theory, we can formulate the maximum entropy approach as a minimization problem involving the objective function,  $Q$ ,

$$Q = \frac{1}{2} \chi^2 - \alpha S, \quad (4)$$

where the usual  $\chi^2$  measure is given by

$$\chi^2 = \sum_{ij} (G_i - \bar{G}_i) [C^{-1}]_{ij} (G_j - \bar{G}_j), \quad (5)$$

where  $\bar{G}_i = G(\tau_i)$  is the Monte Carlo data and  $C_{ij}$  is a covariance matrix element describing the correlation between data,  $\bar{G}_i$  and  $\bar{G}_j$ . The entropy  $S$  is defined by

$$S[A, m] = \int d\omega \{ I(\omega) - m(\omega) - I(\omega) \ln [I(\omega)/m(\omega)] \}. \quad (6)$$

The *default model*  $m(\omega)$  should be chosen by the prior knowledge on the solution. The *regularization parameter*  $\alpha$  is removed by the Bryan’s method<sup>23</sup> in this work. If desired, the real time correlation function  $C(t)$  can be obtained by the inverse Fourier transform from  $I(\omega)$ .<sup>24</sup>

Unlike the direct approach, it is very difficult to get the high frequency components of  $I(\omega)$  since the integral kernel  $e^{-\omega\tau}$  is practically zero beyond a certain frequency  $\omega$ . This implies that it is often impossible to get the overtone peaks which are usually in high frequency region and have small intensities. Another drawback of the maximum entropy method is that it often fails to resolve the closely spaced peaks.<sup>17</sup> To overcome these difficulties, some workers have tried the problem-specific default models constructed from the approximate solutions and sum rules. However, for the lineshape function calculations, it is not adequate to use the non-constant default model. The reason is that  $I(\omega)$  is typically composed of several sharp Gaussian peaks and any incorrect default model thus imposes overly severe constraints on the solution. One might try to improve the result by increasing the number of imaginary time data points or improving a numerical integration schemes. Our experience, however, tells us that neither of those attempts change the outcome significantly. The only previously known way to improve the result is to calculate increasingly accurate values for  $G(\tau)$ . Bearing in mind the fact that the variance in Monte Carlo calculation decreases like  $1/\sqrt{N}$  where  $N$  is the number of Monte Carlo samples, such a “brute force” approach may prove somewhat inefficient.

The relation between  $C(t)$  and  $I(\omega)$  [Eq. (1)] is generally true for the complex time,  $t_c = t - i\tau$ , where  $t$  is the real time and  $\tau$  is the imaginary time. Then, Eq. (1) can be explicitly expressed in terms of  $t$ , and  $\tau$ ,

$$F(t, \tau) = \int_{-\infty}^{\infty} e^{-i\omega t} e^{-\omega\tau} I(\omega) d\omega. \quad (7)$$

This is the “Fourier+Laplace” transform. The only modification from Eq. (2) is that the integral kernel changes to  $e^{-i\omega t} e^{-\omega\tau}$ . It is convenient to use the symmetrized version of the lineshape function,  $A(\omega) \equiv (1 + e^{-\beta\hbar\omega}) I(\omega)$ . Using the detailed balance condition,  $I(-\omega) = e^{-\beta\hbar\omega} I(\omega)$ , and the fact that  $F(t, \tau)$  can be complex, we have two equations to be solved simultaneously,

$$\begin{aligned} \text{Re}[F(t, \tau)] &= \int_0^\infty \cos(\omega t) \frac{e^{-(\tau - \beta\hbar/2)\omega} + e^{(\tau - \beta\hbar/2)\omega}}{e^{-\beta\hbar\omega/2} + e^{\beta\hbar\omega/2}} A(\omega) d\omega, \\ \text{Im}[F(t, \tau)] &= \int_0^\infty \sin(\omega t) \frac{e^{(\tau - \beta\hbar/2)\omega} - e^{-(\tau - \beta\hbar/2)\omega}}{e^{-\beta\hbar\omega/2} + e^{\beta\hbar\omega/2}} A(\omega) d\omega. \end{aligned} \quad (8)$$

One can construct two dimensional correlation function surfaces by the appropriate quantum Monte Carlo technique and then use the surfaces as input data in maximum entropy reconstruction scheme. In the conventional maximum entropy method, only  $F(0, \tau) \equiv G(\tau)$  is used as input data. The obvious advantage of the present method is that we have more information on the system. All the data are not independent so that simply adding more data may not improve the result in a linear fashion. In fact,  $\text{Re}[F(t, \tau)]$  and  $\text{Im}[F(t, \tau)]$  are not independent. However, this does not mean information on imaginary part is redundant. Both data are statistically important. The statistical importance of including  $\text{Im}[F(t, \tau)]$  will be demonstrated in the next section. The important fact to be emphasized is that the real and imaginary time data are mutually complementary: using the real time data it is relatively easy to obtain information on the high frequency spectral components, while, conversely, imaginary time data tend to preferentially provide information concerning low frequency spectral components. It is thus quite natural to expect that by using both real and imaginary time data we can achieve an improved result.

### III. NUMERICAL EXAMPLES

In this section, the utility of our idea is numerically demonstrated for a number of simple examples. In the first model, the lineshape function is assumed to have three Gaussians of width  $10 \text{ cm}^{-1}$  centered at  $300 \text{ cm}^{-1}$ ,  $1000 \text{ cm}^{-1}$ , and  $1800 \text{ cm}^{-1}$ , with the relative intensity 0.1, 1, and 0.1. Each number is chosen to try to represent the typical vibrational spectrum of hydrogen atom adsorbed on the transition metal surfaces.<sup>18,25</sup> The  $1000 \text{ cm}^{-1}$  and  $1800 \text{ cm}^{-1}$  peaks are representative of the perpendicular vibrational motion of the H atom (fundamental and overtone peak), while the peak characteristic of the  $300 \text{ cm}^{-1}$  is the contribution of metal phonon modes. The time correlation functions,  $F(t, \tau)$ , are constructed from  $A(\omega)$  and corrupted by Gaussian noise to simulate the effects of Monte Carlo construction.  $A(\omega)$ ,  $G(\tau)$ , and the real part of  $C(t)$  are shown in Fig. 1. The temperature is set to 100 K.

Figure 2 shows the reconstructed  $A(\omega)$  obtained solely from imaginary time [ $G(\tau)$ ] data with various noise levels. 64 imaginary time data points are included in the calculations. We can see that the proper  $A(\omega)$  is achieved only in the zero error limit. We also notice that, as expected, it is much more difficult to get the small peak at high frequency region than the peak at low frequency region using only the imaginary time data.

The same  $I(\omega)$  reconstructed from purely real time [ $C(t)$ ] data by the conventional numerical Fourier transform and the maximum entropy method is shown in Fig. 3 as a function of  $t_{\text{max}}$ . The real time data are taken at every 1 fs. In the conventional Fourier transform method, we have used

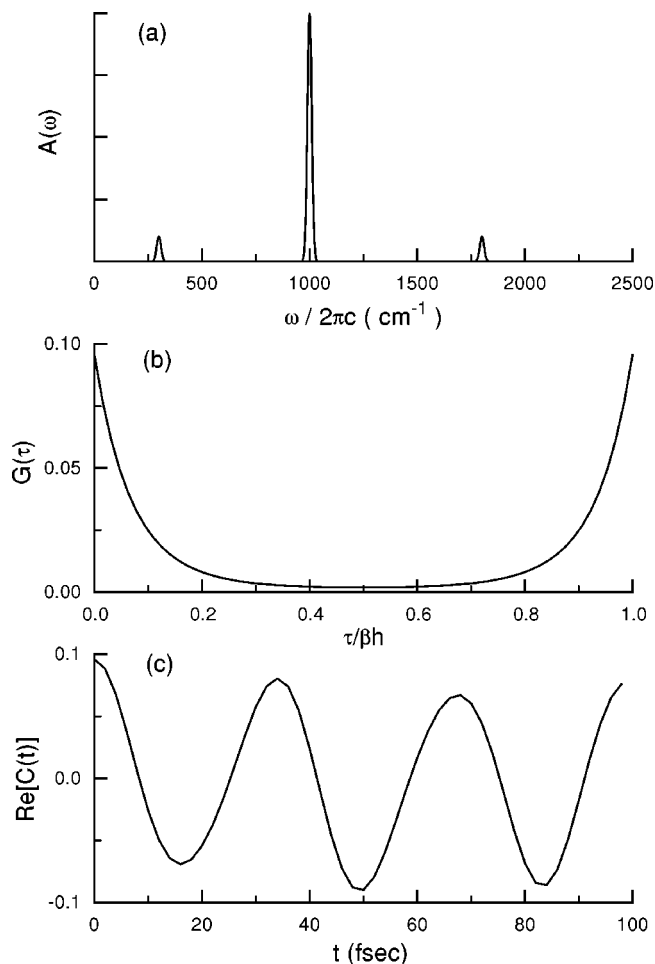


FIG. 1. (a) The first model lineshape function  $A(\omega)$ . (b) Imaginary time position correlation function  $G(\tau)$  computed from  $A(\omega)$  by Laplace transform. The temperature  $T=100 \text{ K}$ . (c) Real part of the real time position correlation function  $\text{Re}[C(t)]$  computed from  $A(\omega)$  by Fourier transform.

the windowing function,  $w(t) = 0.42 + 0.5 \cos(\pi t/t_{\text{max}}) + 0.08 \cos(2\pi t/t_{\text{max}})$  to prevent the error due to the finite time truncation of  $C(t)$ .<sup>22</sup> The maximum entropy method shows superior performance over the usual Fourier transform method. As expected, relatively long time information is needed to correctly locate the low frequency peak. We want to emphasize again the fact that the correct spectrum can be

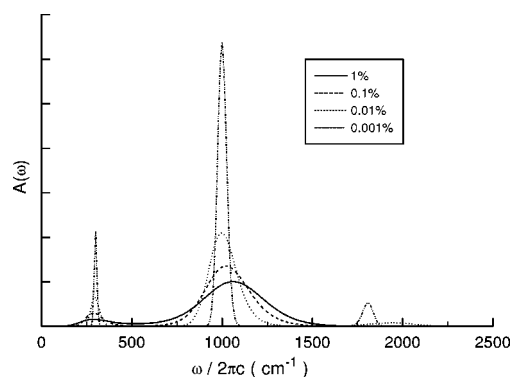


FIG. 2. Lineshape functions extracted from  $G(\tau)$  data for Fig. 1 using maximum entropy method. Each  $G(\tau)$  is corrupted by 1%, 0.1%, 0.01%, and 0.001% (relative to maximum value) unbiased Gaussian noises.

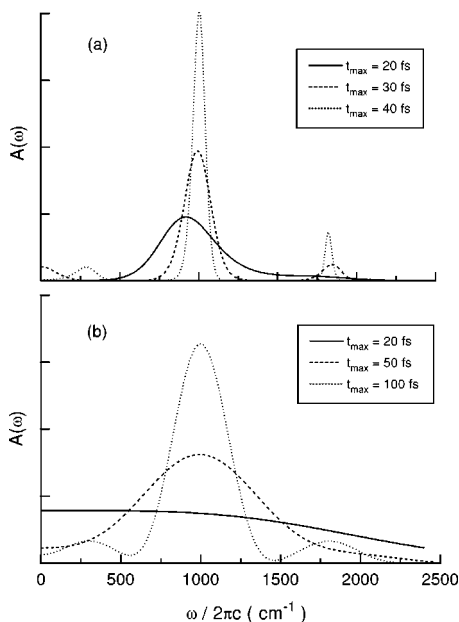


FIG. 3. Lineshape functions  $A(\omega)$  extracted from  $\text{Re}[C(t)]$  data as a function of  $t_{\text{max}}$ .  $\text{Re}[C(t)]$  is corrupted by the Gaussian noise whose size is 1% of the maximum value of  $\text{Re}[C(t)]$ . (a)  $A(\omega)$  obtained by maximum entropy method. (b)  $A(\omega)$  obtained by the conventional numerical Fourier transform with the windowing function  $w(t) = 0.42 + 0.5 \cos(\pi t/t_{\text{max}}) + 0.08 \cos(2\pi t/t_{\text{max}})$ .

obtained only at the zero error limit for  $G(\tau)$  case or long time limit for  $C(t)$  case and that it is extremely hard or time-consuming to approach either of these two limits.

The complementary properties of  $G(\tau)$  and  $C(t)$  are clearly illustrated in Fig. 4 which shows the lineshape functions calculated by maximum entropy method using the various data sets, (i)  $G(\tau)$ , (ii)  $\text{Re}[C(t)]$ , (iii)  $G(\tau) + \text{Re}[C(t)]$ , and (iv)  $G(\tau) + \text{Re}[C(t)] + \text{Im}[C(t)]$ , where  $\text{Re}[C(t)]$  and  $\text{Im}[C(t)]$  are the real and imaginary part of  $C(t)$ . The main peaks are reasonably reproduced for all the cases, but cases (i) and (ii) fail to capture the small peak at either high frequency side or low frequency side. If  $G(\tau)$  and  $C(t)$  together are fed into the maximum entropy method as input data, two minor peaks at both sides are successfully located at the correct positions. We also see that case (iv) performs

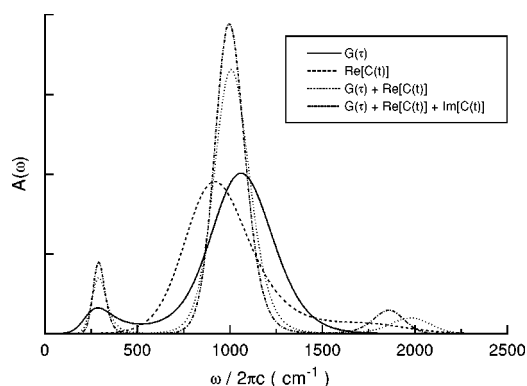


FIG. 4. Lineshape functions  $A(\omega)$  extracted from the various data sets. 1% relative Gaussian noises are added to  $G(\tau)$  and the Gaussian noises of 1% relative to the maximum value of  $C(t)$  are added to  $C(t)$ .  $t_{\text{max}} = 20$  fs.

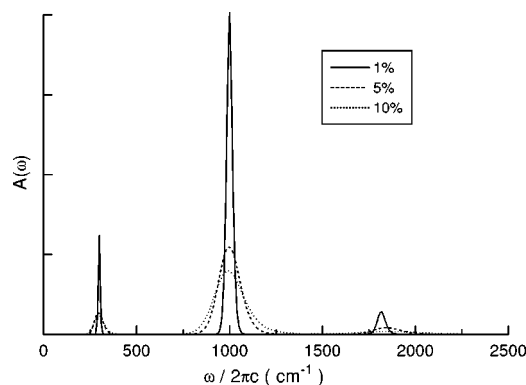


FIG. 5. Lineshape functions  $A(\omega)$  extracted from  $F(t, \tau)$ . Two dimensional real and imaginary parts of  $F(t, \tau)$  have been used.  $t_{\text{max}} = 20$  fs. The noise levels are 1%, 5%, and 10% of the maximum value of  $F(t, \tau)$  for each  $t$ .

better than case (iii), which indicates the statistical importance of including the imaginary part of the real time data. The best result can be obtained if we use all the data available which include the real and imaginary parts of  $F(t, \tau)$  on 2-D complex plane (see Fig. 5). There is no special difficulty in calculating  $C(t)$  from  $A(\omega)$  using the Fourier transform, since  $A(\omega)$  is numerically complete.  $\text{Re}[C(t)]$  obtained from  $A(\omega)$  is shown in Fig. 6 which demonstrates the ability of the method to “predict” the real time correlation function only using the imaginary time data and the short time data.

The second model is composed of two closely spaced Gaussian peaks of width  $10 \text{ cm}^{-1}$  centered at  $800 \text{ cm}^{-1}$  and  $1000 \text{ cm}^{-1}$ , with the same intensities. They may be thought as the parallel and perpendicular vibrational modes of the adsorbed hydrogen atom on the metal surface.<sup>25</sup> The results are similar to those of the first model. That is, the inclusion of the real time data greatly improves the quality of the lineshape function calculation, relative to that achievable using imaginary time data alone (see Fig. 7).

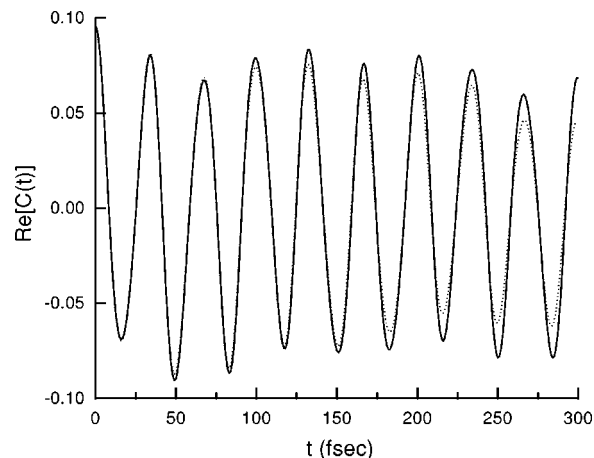


FIG. 6. The real part of the real time correlation function  $\text{Re}[C(t)]$  obtained from  $I(\omega)$  by numerical Fourier transform.  $I(\omega)$  for 1% noise level case in Fig. 5 has been used for the calculation. The exact  $\text{Re}[C(t)]$  (solid line) is also plotted for comparison.

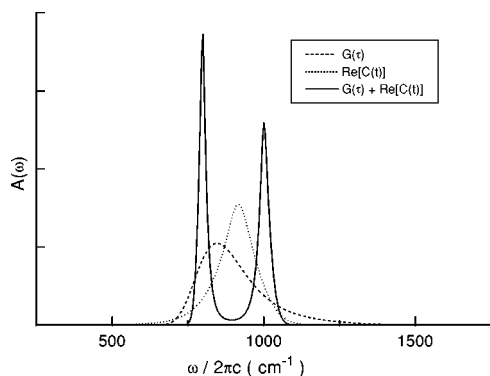


FIG. 7. Lineshape functions  $A(\omega)$  for the second model extracted from the various data sets. The exact  $A(\omega)$  has two Gaussians of width  $10 \text{ cm}^{-1}$  centered at  $800 \text{ cm}^{-1}$  and  $1000 \text{ cm}^{-1}$  with the same intensity. 1% relative Gaussian noises are added to  $G(\tau)$  and the Gaussian noises of 1% relative to the maximum value of  $C(t)$  are added to  $C(t)$ .  $t_{\text{max}} = 20 \text{ fs}$ .

#### IV. CONCLUSIONS

In this paper, we have developed the new numerical method based on the maximum entropy method to investigate the finite temperature quantum dynamics problems. The method is based on the complementary nature of the imaginary and real time information on the quantum system. Once the time correlation function as a function of the imaginary time  $\tau$  and the real time  $t$  has been expressed in terms of a Fourier and Laplace transform of the spectral density, then it is possible to use the maximum entropy method in a straightforward manner. We have demonstrated the advantages of our new method for two examples representative of adsorbate vibrational lineshapes of metal/hydrogen systems. We have found that ‘‘limited’’ real time information greatly improves the usual maximum entropy scheme. By ‘‘limited’’ we generally mean information realistically available from direct Monte Carlo methods. For our model studies, 20 fs is roughly the time required to capture reasonably good results. 20 fs is about half of one vibrational period for both examples. Because the temperature is taken to be 100 K,  $20 \text{ fs}/\beta\hbar$  is about 0.3.

The ultimate utility of the method depends on how far and how accurately we can get the real time information and the expense of the real time quantum Monte Carlo calculations. We argue that the present results suggest that it may

prove computationally more efficient to include real time data than exclusively adding Monte Carlo sampling points to improve the imaginary time data. The new method appears especially useful for systems whose lineshape functions have small components in both of low and high frequency regions. Based on our experience with the maximum entropy method, the statistical independence of the input data is very important. We thus want to point out that any Monte Carlo scheme that introduces bias to the data may not be suitable to the maximum entropy method.

#### ACKNOWLEDGMENTS

The authors wish to thank J. Gubernatis for introducing us to the maximum entropy method and helpful discussions. The authors wish to acknowledge support through NSF Grants Nos. CHE-9411000 and CHE-9625498.

- <sup>1</sup>N. Metropolis and S. Ulam, *J. Am. Stat. Assoc.* **44**, 335 (1949).
- <sup>2</sup>M. H. Kalos and P. A. Whitlock, *Monte Carlo Methods* (Wiley-Interscience, New York, 1986).
- <sup>3</sup>J. D. Doll, D. L. Freeman, and T. L. Beck, *Adv. Chem. Phys.* **78**, 61 (1990).
- <sup>4</sup>B. J. Berne and D. Thirumalai, *Annu. Rev. Phys. Chem.* **47**, 401 (1986).
- <sup>5</sup>D. Thirumalai and B. J. Berne, *Comput. Phys. Commun.* **63**, 415 (1991).
- <sup>6</sup>E. C. Behrman and P. G. Wolynes, *J. Chem. Phys.* **83**, 5863 (1985).
- <sup>7</sup>V. S. Filinov, *Nucl. Phys. B* **271**, 717 (1986).
- <sup>8</sup>J. D. Doll, T. L. Beck, and D. L. Freeman, *J. Chem. Phys.* **89**, 5753 (1988).
- <sup>9</sup>N. Makri and W. H. Miller, *J. Chem. Phys.* **89**, 2170 (1988).
- <sup>10</sup>C. H. Mak, *Phys. Rev. Lett.* **68**, 899 (1992).
- <sup>11</sup>G. Baym and N. D. Mermin, *J. Math. Phys.* **2**, 232 (1961).
- <sup>12</sup>H.-B. Schüttler and D. J. Scalapino, *Phys. Rev. Lett.* **55**, 1204 (1985).
- <sup>13</sup>M. Jarrell and O. Biham, *Phys. Rev. Lett.* **63**, 2504 (1989).
- <sup>14</sup>J. E. Gubernatis, M. Jarrell, R. N. Silver, and D. S. Sivia, *Phys. Rev. B* **44**, 6011 (1991).
- <sup>15</sup>M. Jarrell and J. E. Gubernatis, *Phys. Rep.* **269**, 133 (1996).
- <sup>16</sup>E. Gallicchio and B. J. Berne, *J. Chem. Phys.* **101**, 9909 (1994).
- <sup>17</sup>M. Boninsegni and D. M. Ceperley, *J. Low Temp. Phys.* **104**, 339 (1996).
- <sup>18</sup>D. Kim, J. D. Doll, and J. E. Gubernatis, *J. Chem. Phys.* **106**, 1641 (1997).
- <sup>19</sup>D. A. McQuarrie, *Statistical Mechanics* (Harper and Row, New York, 1976).
- <sup>20</sup>R. P. Feynman and A. R. Hibbs, *Quantum Mechanics and Path Integrals* (McGraw-Hill, New York, 1965).
- <sup>21</sup>R. P. Feynman, *Statistical Mechanics* (Academic, New York, 1972).
- <sup>22</sup>M. P. Allen and D. J. Tildesley, *Computer Simulations of Liquid* (Oxford Science, Oxford, 1987).
- <sup>23</sup>R. K. Bryan, *Eur. Biophys. J.* **18**, 165 (1990).
- <sup>24</sup>J. Bonca and J. E. Gubernatis, *Phys. Rev. E* **53**, 6504 (1996).
- <sup>25</sup>K. J. Maynard, A. D. Johnson, S. P. Daley, and S. T. Ceyer, *Faraday Discuss. Chem. Soc.* **91**, 437 (1991).